Biochemical and Biophysical Research Communications 405 (2011) 24–30

Contents lists available at ScienceDirect

Biochemical and Biophysical Research Communications

journal homepage: www.elsevier.com/locate/ybbrc

Solution structure of UIM and interaction of tandem ubiquitin binding domains in STAM1 with ubiquitin

Jongsoo Lim [a,b], Woo-Sung Son [c], Joon Kyu Park [d], Eunice EunKyeong Kim [d], Bong-Jin Lee [e], Hee-Chul Ahn [a,b,*]

[a] Biomolecular Science, University of Science and Technology, Daejeon 305-350, Republic of Korea
[b] Advanced Analysis Center, Korea Institute of Science and Technology, Seoul 136-791, Republic of Korea
[c] Department of Pharmacy, CHA University, Gyeonggi-do 487-801, Republic of Korea
[d] Biomedical Center, Korea Institute of Science and Technology, Seoul 36-791, Republic of Korea
[e] Research Institute of Pharmaceutical Sciences, College of Pharmacy, Seoul National University, Seoul 151-742, Republic of Korea

ARTICLE INFO

Article history:
Received 14 December 2010
Available online 25 December 2010

Keywords:
Ubiquitin
STAM1
ESCRT
Lysosomal degradation
UIM
VHS
NMR
ITC

ABSTRACT

STAM1 and Hrs are the components of ESCRT-0 complex for lysosomal degradation of membrane proteins is composed of STAM1 Hrs and has multiple ubiquitin binding domains. Here, the solution structure of STAM1 UIM, one of the ubiquitin binding motif, was determined by NMR spectroscopy. The structure of UIM adopts an α-helix with amphipathic nature. The central hydrophobic residues in UIM provides the binding surface for ubiquitin binding and are flanked with positively and negatively charged residues on both sides. The docking model of STAM1 UIM-ubiquitin complex is suggested. In NMR and ITC experiments with the specifically designed mutant proteins, we investigated the ubiquitin interaction of tandem ubiquitin binding domains from STAM1. The ubiquitin binding affinity of the VHS domain and UIM in STAM1 was 52.4 and 94.9 μM, and 1.5 and 2.2 fold increased, respectively, than the value obtained from the isolated domain or peptide. The binding affinities here would be more physiologically relevant and provide more precise understanding in ESCRT pathway of lysosomal degradation.

1. Introduction

The ubiquitination of proteins is one of the widespread post-translational modifications and regulates a variety of cellular processes [1]. Protein modification by ubiquitin can be achieved through the formation of an isopeptide bond between the carboxyl group of the C-terminal glycine of ubiquitin and an ε–amino group of a lysine residue from a target protein [2]. The lysine residues on ubiquitin also can be modified by other ubiquitin, resulting in the formation of the polyubiquitin chains. Thus, the ubiquitinated target proteins are found in several ways, such as monoubiquitinated, multiple monoubiquitinated, and polyubiquitinated forms. The type of ubiquitination of target protein is related to the fate of the protein in various cellular processes. For example, it was reported that monoubiquitination is involved in endocytosis [3–5]. K48-linked polyubiquitination is very well characterized and the signal for the proteasomal degradation pathway [reviewed in Ref. 6], whereas recent evidences revealed that multiple monoubiquitinantion or K63-linked polyubiquitination is the sorting signal in the lysosomal degradation of membrane proteins [7,8].

Ubiquitin-mediated selective trafficking of membrane proteins for lysosomal degradation is crucial for quality control in the cell and proper cell signaling. Ubiquitinated membrane proteins should be delivered inside of the cell via multivesicular bodies (MVBs) by endocytosis, and finally to lysosomes. The endosomal sorting complex required for transport (ESCRT) complexes sort the ubiquitinated membrane proteins for lysosomal degradation [reviewed in Ref. 9]. The signal transducing adaptor molecule (STAM) and hepatocyte growth factor-regulated substrate (Hrs) constitute the ESCRT-0 complex to sort the ubiquitinated cargo proteins from the early endosomes to the ESCRT-1 complex [10,11]. Interestingly, the ESCRT-0 complex contains multiple ubiquitin binding domains, a Vps27/ Hrs/Stam (VHS) domain and a ubiquitin binding motif (UIM) for STAM, and a VHS domain and a double-sided ubiquitin interacting motif (DUIM) for Hrs, respectively. Via those multiple ubiquitin binding domains, ESCRT-0 recognizes ubiquitinated cargo proteins, in which the VHS domain of STAM has higher binding affinity to K63-linked diubiquitin than to K48-linked diubuquitin

Abbreviations: MVB, multivesicular body; ESCRT, endosomal sorting complex required for transport; STAM, signal transducing adaptor molecule; Hrs, hepatocyte growth factor-regulated substrate; VHS, Vps7/Hrs/Stam; UIM, ubiquitin interacting motif; DUIM, double-sided ubiquitin interacting motif; $STAM1^{N191}$, N-terminal 191 amino acids of STAM1; NOESY, nuclear Overhause effect spectroscopy; TOCSY, total correlation spectroscopy; DQF-COSY, double quantum filtered correlation spectroscopy; HSQC, heteronuclear single quantum correlation; CSP, chemical shift perturbation; ITC, isothermal titration calorimetry.

* Corresponding author. Address: Advanced Analysis Center, Korea Institute of Science and Technology, 39-1 Hawolgok-dong, Seoungbuk-gu, Seoul 136-791, Republic of Korea. Fax: +82 2 958 5969.
E-mail addresses: hcahn@kist.re.kr, heechulahn@gmail.com (H.-C. Ahn).

0006-291X/$ - see front matter © 2010 Elsevier Inc. All rights reserved.
doi:10.1016/j.bbrc.2010.12.103

[12,13]. Recently, Ren and Hurley suggested that the preference of ESCRT-0 to K63-linked tetraubiquitin over monoubiquitin should be attributed to the cooperation of flexibly connected VHS and UIM motifs of ESCRT-0 [12].

To investigate the binding preference of ESCRT-0 to K63-linked di-, or poly-ubiquitin, it is pre-requisite to understand both individual VHS-ubiquitin and UIM-ubiquitin interactions. Previously, we determined a novel ubiquitin binding site on STAM1 VHS and suggested the mode of VHS-ubiquitin interaction by using NMR spectroscopy [14]. We also reported the result of backbone resonance assignments for N-terminal 191 amino acids of STAM1 ($STAM1^{N191}$) which contain both VHS and UIM [15]. In this work, we present the solution structure of STAM1 UIM and the interaction between the UIM motif and ubiquitin. By using the mutant protein of $STAM1^{N191}$, we evaluated the affinities for ubiquitin of the VHS domain and UIM individually.

2. Materials and methods

2.1. Peptide synthesis and protein preparation

The synthetic peptide, KEEEDLAKAIELSLKEQRQQS, corresponding to UIM of STAM1 (Fig. 1A), was purchased from Anygen (Gwangju, Korea). The UIM peptide was dissolved in 20 mM sodium phosphate buffer, pH 6.8, with 1 mM DTT, 0.1 M NaCl, 0.5 mM PMSF, 0.05 mM NaN_3 and 5% (v/v) D_2O for NMR experiments. The concentration of UIM peptide was 2 mM.

The STAM1 protein containing both the VHS domain and UIM was prepared as previously described [15]. The single and double mutant STAM1 proteins, $STAM1^{N191}$W26A, I179G, W26AL176A, W26AI179G, and W26AS183A were prepared by site-directed mutagenesis.

Ubiquitin for NMR and ITC experiments was expressed and purified as described previously [14].

2.2. NMR measurements

All NMR experiments were carried out at 298 K on Varian VNMRS 900 MHz spectrometer with z-axis gradient equipment. For STAM1 UIM, two-dimensional nuclear Overhauser effect spectroscopy (2D NOESY) (mixing times of 120 and 200 ms), total correlation spectroscopy (TOCSY) (mixing times of 60 ms), and double quantum filtered correlation spectroscopy (DQF-COSY) were performed using presaturation of the H_2O resonance by continuous irradiation.

For NMR titration experiments, increasing amount of unlabeled STAM1 UIM peptides, the wild-type $STAM1^{N191}$ were added to ^{15}N-labeled ubiquitin, respectively, and series of 2D $^{1}H–^{15}N$ heteronuclear single quantum correlation (HSQC) spectra were recorded. Reciprocally, unlabeled ubiquitin were titrated into ^{15}N-labeled $STAM1^{N191}$W26A and series of 2D $^{1}H–^{15}N$ HSQC spectra were recorded at various molar ratios. From the NMR titration data, the sites of protein–protein interaction were determined based on the chemical shift perturbation (CSP) plot versus the protein sequences, where CSP was calculated by using the formula, $CSP = [(\Delta H)^2 + (\Delta N/6.51)^2]^{1/2}$.

All NMR data were processed using NMRPipe software [16] and were analyzed using NMRView software [17].

2.3. Structure calculation of STAM1 UIM

The spin systems of STAM1 UIM were identified from the TOCSY and DQF-COSY spectra, and the sequential assignments were unambiguously accomplished from the analysis of the NOESY spectra by the conventional method [18]. The NOE-based distance restraints were derived based on the peak volume by using the program ARIA 2.0 [19]. The backbone dihedral angle restraints were obtained from the analysis of DQF-COSY spectrum. The peptide structures were calculated by using the program ARIA 2.0 and CNS 1.2 [20] with 160 distance restraints and 30 dihedral angle restraints (Table 1). Twenty-six hydrogen bond restraints were incorporated into the final calculation of the peptide structures based on the secondary structure of UIM. In the final ARIA run, 100 structures were calculated and the 20 lowest energy structures were selected for statistical analysis by using PROCHECK-NMR 3.4 [21].

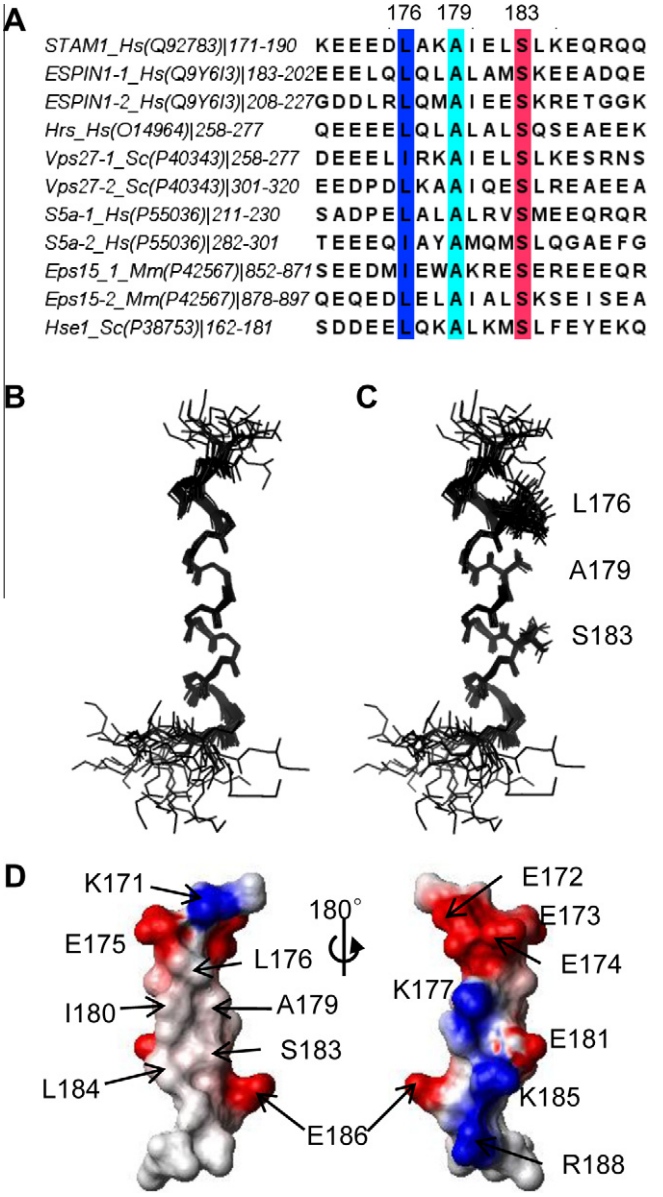

Fig. 1. (A) Sequence alignment of UIM. The highly conserved hydrophobic residues are indicated in color. (B) Energy lowest 20 ensemble structures of STAM1 UIM. (C) Conformation of side-chains from the conserved hydrophobic residues. (D) Electrostatic potential presentation of STAM1 UIM. The hydrophobic surfaces are colored in gray, and the positively and negatively charged surfaces are shown in blue and red, respectively. Throughout the figure, one-letter amino acid codes are used with the sequence number of STAM1. (For interpretation of references to color in this figure legend, the reader is referred to the web version of this article.)

2.4. Isothermal titration calorimetry

ITC measurements were carried out by using ITC-200 microcalorimeter (MicroCal, Northampton, MA). The same buffer for NMR

Table 1
Structural statistics for the final 20 structures of STAM1 UIM.

Number of experimental restraints	
NOE distance restraints	167
Hydrogen bond restraints	26
Torsion angle restraints	30
Number of violations	
NOE > 0.3 (Å)	0
Dihedral angle > 0.5 (°)	0
Energies (kcal/mol)	
E_{total}	−791.54 ± 45.06
E_{bond}	0.25 ± 0.01
E_{angle}	8.51 ± 0.11
$E_{improper}$	0.30 ± 0.01
E_{dihed}	93.67 ± 1.01
E_{vdw}	−157.20 ± 2.09
E_{elec}	−737.37 ± 45.70
E_{NOE}	0.63 ± 0.46
RMSD from experimental restraints	
NOE (Å)	0.008 ± 0.003
Torsion angle (°)	0.021 ± 0.038
RMSD from the idealized gemometry	
Bonds (Å)	0.001 ± 0.000
Bond angles (°)	0.296 ± 0.002
Improper angles (°)	0.111 ± 0.010
Ramachandran plot (%)[a]	
Most favored	85.5
Additionally allowed	12.9
Generously allowed	1.1
Disallowed[b]	0.5
RMSD of well-ordered region (Å)[c]	
Backbone	0.33
Heavy atoms	1.28

[a] As determined by PROCHECK-NMR.
[b] Disallowed regions were from the unstructured region.
[c] RMSD was calculated by using the software MOLMOL [30] for the well-ordered residues of STAM1 UIM (Glu3–Gln17).

measurements without D_2O was used. Aliquots of 3 mM ubiquitin were added at an interval of 150 s to the wild-type and mutant STAM1 protein solutions (0.1 mM) in the cell with gentle stirring using computer-controlled micro-syringe. The binding stoichiometry and binding constants were calculated by fitting the data to one site binding model using MicroCal Origin (version 7.0) software.

3. Results

3.1. Solution structure of STAM1 UIM

The three-dimensional structure of the synthetic STAM1 UIM peptide was determined by NMR spectroscopy. As shown in Fig. 1, STAM1 UIM adopts a single α-helix spanning from Glu173 to Gln187 in aqueous solution. The 20 lowest energy structures of STAM1 UIM were well converged with the backbone rmsd of 0.33 Å for the helical region (Fig 1B). Based on the sequence homology between various UIMs (Fig 1A), the conserved residues, Leu176, Ala179, and Ser183, are presented with the sidechain configurations (Fig 1C). The surface charge potential presents the amphipathic nature of STAM1 UIM (Fig. 1D). The hydrophobic residues are on one surface of STAM1 UIM, while the positively and negatively charged residues are on the other side of UIM helix.

3.2. Interaction between ubiquitin and STAM1 UIM peptide

To determine the UIM binding surface on ubiquitin, NMR titration experiments were carried out. The ^{15}N-labeled ubiquitin samples were prepared and titrated with increasing amount of STAM1 UIM peptide. Fig. 2A shows the overlaid $^{1}H–^{15}N$ HSQC spectra of ubiquitin at various molar ratios of UIM to ubiquitin. Most of the $^{1}H–^{15}N$ resonances from ubiquitin residues were not changed by the addition of STAM1 UIM, however, some of the resonances were significantly perturbed. Those are Thr7, Leu8, Ile13, Arg42, Leu43, Ile44, Phe45, Ala46, Gly47, Lys48, Gln49, Leu71, and Leu73. Especially, the resonance of Ala46 was significantly line-broadened and disappeared even at 0.2 M ratio of the added STAM1 UIM to ubiquitin. The magnitude of the chemical shift perturbation by the addition of STAM1 UIM to ubiquitin is summarized in Fig. 2B, where the line-broadened Ala46 is indicated by the gray bar with the maximal perturbation value for the clarity of understanding. The ubiquitin residues involved in UIM binding are sequestered on the same surface of ubiquitin except for the residue Ile13 (Fig. 2E). Ile13 and Thr14 of ubiquitin are not involved in the direct contact with UIM, however, those two residues frequently showed the chemical shift perturbation upon the addition of several ubiquitin binding domains [22]. In our previous report [14] as well as in this work (Fig. 2C, D), the resonances of Ile13 and Thr14 were perturbed significantly because of the conformational change by the addition of STAM1. The UIM binding surface determined in this work corresponds well with that of previous works [22–24].

3.3. Interaction between ubiquitin and STAM1^{N191}

NMR titration experiments were also carried out by using ^{15}N-labeled ubiquitin with unlabeled STAM1^{N191}. Since STAM1^{N191} contains two ubiquitin binding units, the VHS domain and UIM, the manner of the chemical shift perturbation for the ubiquitin-STAM1^{N191} complex was slightly different from that of the ubiquitin-STAM1 UIM (Fig. 2C). The $^{1}H–^{15}N$ resonances of Leu8, Ile44, Gly47, Gln49 as well as Ala46 which showed significant line-broadening with the addition of UIM, were disappeared at the STAM1^{N191} to ubiquitin molar ratio of 2. The degree of perturbation by the addition of STAM1^{N191} to ubiquitin (Fig. 2D) was more severe than that in the STAM1 UIM-ubiquitin complex (Fig. 2B).

3.4. Effect of UIM in STAM1 for ubiquitin binding

To evaluate the effect of UIM in STAM1 for ubiquitin binding, Trp26 of STAM1 was substituted with alanine to eliminate the binding affinity of the VHS domain to ubiquitin and the ^{15}N-labeled W26A mutant of STAM1^{N191} was subjected to the NMR titration experiments. Since previous reports provided that Trp26 in the VHS domain is the key residue in ubiquitin binding, the mutation of tryptophan to alanine resulted in the complete loss of binding affinity to ubiquitin [12,14]. Thus, the ubiquitin binding of STAM1^{N191}W26A should be attributed to the UIM motif. As expected, the titration of unlabeled ubiquitin perturbed only the resonances from UIM of ^{15}N-labeled STAM1^{N191} (Fig. 3A). The STAM1 resonances from the residues, Ala168, Lys171, Glu174, Asn175, Leu176, Lys178, Ser183, Glu186, Gln187, and Arg188 showed significant chemical shift perturbation. The $^{1}H–^{15}N$ resonances from Glu172, Glu173, Ala177, Ala179-Leu182, Leu184, and Lys185 were line-broadened and disappeared in the presence of 6 M excess ubiquitin. The summarized perturbation plot versus the STAM1 sequence in Fig. 3B clearly shows the contribution of UIM alone in ubiquitin binding.

We also titrated ubiquitin to ^{15}N-labeled wild-type STAM1^{N191}. From $^{1}H–^{15}N$ HSQC spectra of ^{15}N-labeled STAM1 with ubiquitin, the binding of STAM1 VHS as well as UIM to ubiquitin were detected (Supplementary Fig. S1). The CSP plot of ubiquitin binding to STAM1^{N191} (Supplementary Fig.S1B) showed the identical pattern to our previous work (CSP plot of VHS with ubiquitin in Ref. [14]) for the VHS domain and to this work for UIM (Fig. 3B), suggesting the simultaneous ubiquitin binding of VHS and UIM in intact STAM1.

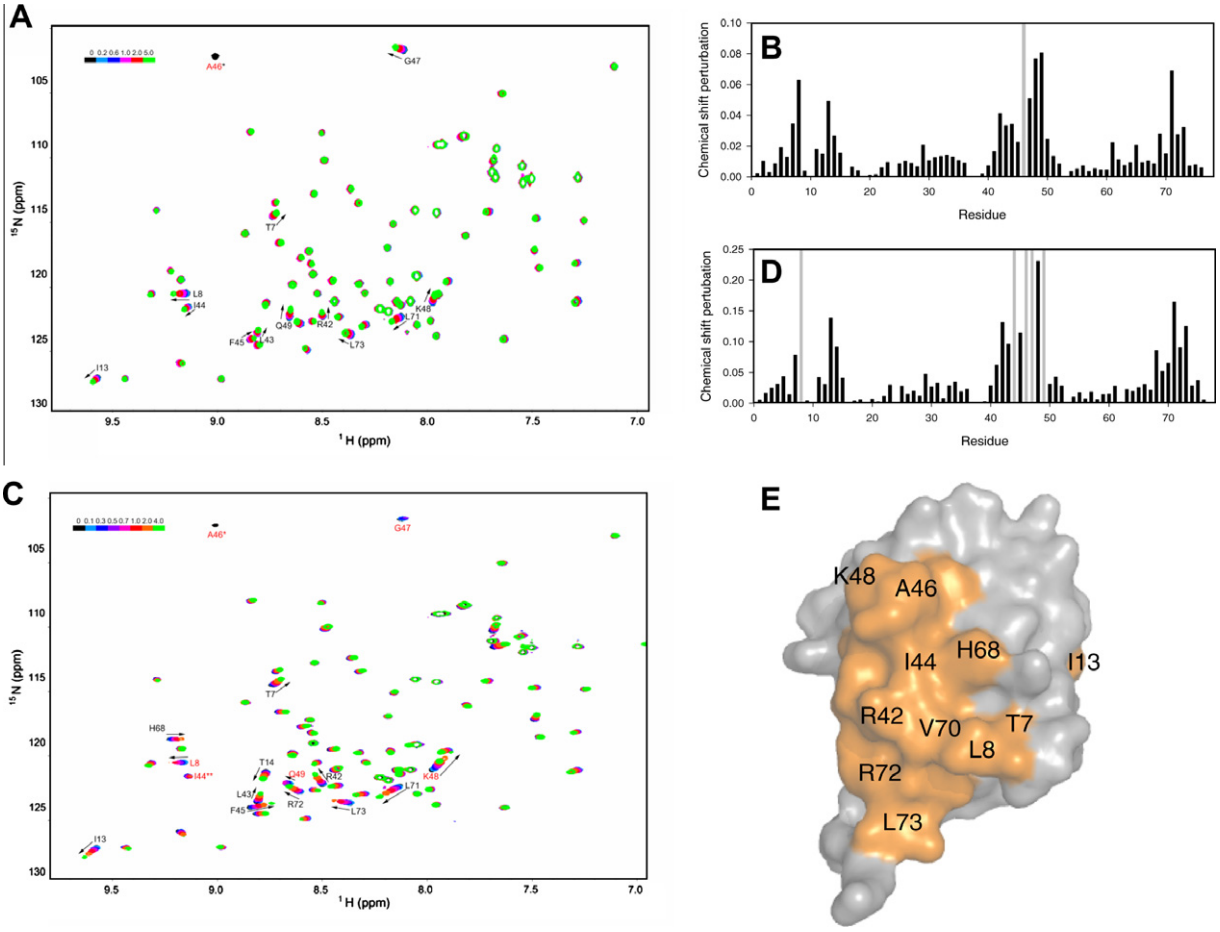

Fig. 2. STAM1 UIM binding site on ubiquitin. Overlaid ^{1}H–^{15}N HSQC spectra of ubiquitin (A and C) and CSP plot (B and D) upon the addition of STAM1 UIM peptide and STAM1^{N191}, respectively. The molar ratios of UIM to ubiquitin are indicated by color bars on the spectra (A and C). The resonances perturbed significantly are labeled with amino acid codes and arrows. The line-broadened residues during NMR titration are colored in red and indicated by gray bars with maximal value in CSP plots. (E) Consensus UIM binding surface of ubiquitin from NMR titration experiments. (For interpretation of references to color in this figure legend, the reader is referred to the web version of this article.)

3.5. Ubiquitin binding affinity of STAM1^{N191}

To measure the individual ubiquitin binding affinity of the VHS domain and UIM from STAM1, the isothermal titration calorimetry was performed with the specifically designed mutant STAM1 proteins. Initially the synthetic STAM1 UIM peptide was titrated to ubiquitin, however, it did not give rise to any binding information because the raw data of ITC experiments presented too low heat exchange upon titration (data not shown). Therefore, we used the mutant STAM1 proteins for ITC experiments.

To evaluate the ubiquitin binding affinity of the VHS domain in STAM1, the A179G mutant protein was used, since Ala179 was reported as the key residue for ubiquitin binding in UIM [22]. On the other hand, to evaluate the affinity of UIM of STAM1 to ubiquitin, the W26A mutant was used.

All data were fitted by using the one-site binding model, even though the wild-type STAM1^{N191} contains two ubiquitin binding sites, the VHS domain and UIM, since two-side binding model was not well fitted. In one-site binding model, the dissociation constant between STAM1^{N191} and ubiquitin was 52.4 ± 8 μM with the stoichiometry parameter, n = 2.08, which suggest STAM1^{N191} binds two ubiquitin molecules (Fig. 4A). The dissociation constant of STAM1^{N191}I179G (effect of VHS) with ubiquitin was 28.7 ± 6 μM with n = 1.33, suggesting the contribution of the VHS domain alone in STAM1 to ubiquitin. This affinity between the VHS domain and ubiquitin is somewhat elevated value compared to the previous report [12,14]. The affinity of UIM alone in STAM1 (STAM1^{N191}W26A) to ubiquitin, 94.9 ± 8 μM (n = 0.98) was also higher than the reported value measured with the synthetic STAM1 UIM peptide [22]. It is not clear what would be the cause of the elevation of the ubiquitin binding affinity with the larger polypeptide than in the isolated domain or peptide. One possible explanation would be that the more restricted diffusion of the larger polypeptide, the STAM1^{N191} mutants, in solution would increase the effective local concentration of the proteins surrounding ubiquitins, which would result in the higher affinity than the isolated domain or peptide motif. Indeed, Fisher et al. [22] showed STAM1 UIM with flanking sequences has slightly enhanced affinity to ubiquitin than UIM itself. In this study, the affinity to ubiquitin was increased by 1.5 and 2.2 fold for the VHS domain and UIM in the intact STAM1, respectively, compared to the isolated domain or peptide.

3.6. Role of hydrophobic residues in ubiquitin binding

Three double mutants, STAM1^{N191}W26AL176A, STAM1^{N191}W26AA179G, and STAM1^{N191}W26AS183A were produced and used to investigate the role of the conserved residues, Leu176, Ala179, and Ser183, which provide the hydrophobic surface to bind ubiquitin (Fig. 1A). The selection of three hydrophobic residues, Leu176, Ala179, and Ser183, was made based on following reasons: (1) the central alanine and serine in UIM (Ala179 and Ser183 for STAM1) play key role in the interaction with the hydrophobic surface cen-

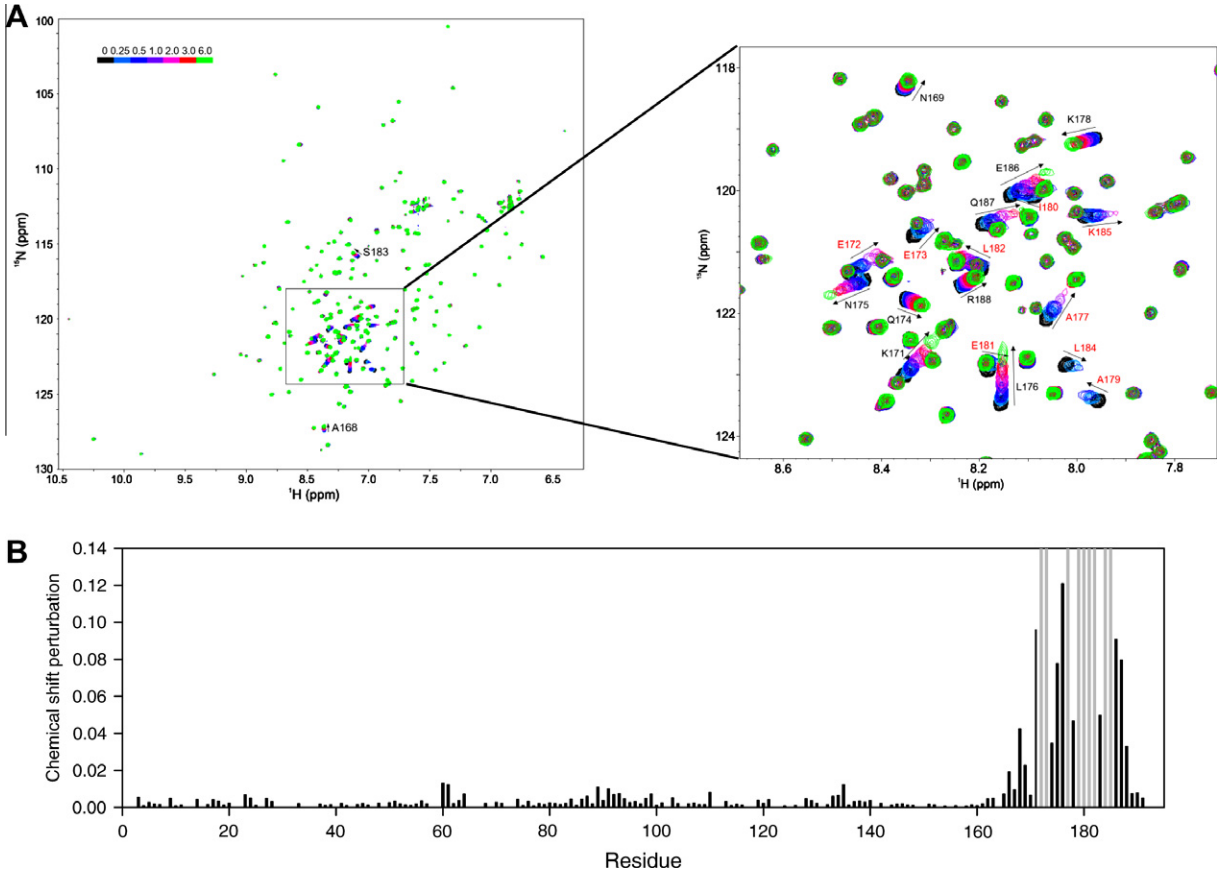

Fig. 3. Ubiquitin binding site on STAM1 UIM. (A) Overlaid $^{1}H–^{15}N$ HSQC spectra of STAM1^{N191}W26A with increasing amount of ubiquitin. The color bars on the spectrum indicate the molar ratios of STAM1^{N191}W26A to ubiquitin. The crowd region in the spectra is enlarged. (B) CSP plot to determine ubiquitin binding site of STAM1. The line-broadened residues during NMR titration are colored in red (A) and indicated by gray bars with maximal value in CSP plots (B). (For interpretation of references to color in this figure legend, the reader is referred to the web version of this article.)

tered at Ile44 of ubiquitin [22,25], and (2) Leu176 is also one of the most conserved residues and is exactly on the extended surface provided by Ala179 and Ser183, while other hydrophobic residues, such as Ileu180 and Leu184, are less conserved and provide another plane of the hydrophobic surface of STAM1 UIM (Fig. 1).

As expected, STAM1^{N191}W26AA179G and W26AS183A lost ubiquitin binding affinity, even though STAM1^{N191}W26AA179G retained very weak but undetectable affinity (Fig. 4E and F). The mutation of leucine to alanine at the residue 176 resulted in the complete loss of ubiquitin binding affinity (Fig. 4D). Thus, the ubiquitin binding of STAM1 UIM should be attributed to the conserved hydrophobic residues.

4. Discussion

ESCRT complexes sort the ubiqutinated membrane cargo proteins for lysosomal degradation, where STAM and Hrs is the component of ESCRT-0 complex and mediate the sorting of the ubiquitinated cargo proteins from the early endosomes to the ESCRT-1 complex [10,11]. Interesting feature of ESCRT-0 is the presence of multiple ubiquitin binding domains, and via these domains ESCRT-0 would recognize multiple monoubiquitins or polyubiquitin in membrane protein trafficking. Recently, Ren and Hurley showed that ESCRT-0 binds K63-linked tetraubiquitin 50-fold more tightly than monoubiquitin and the gain in affinity should be attributed to cooperation of flexibly connected VHS and UIM motifs [12]. Lange et al. suggested different mode of binding of STAM2 VHS for K48- and K63-linked diubiquitin and the preference of VHS for K63-linked diubiquitin [13]. Even with those recent evidences, the exact molecular and structural bases why ESCRT-0 components prefer K63-linked polyubiquitin are still of great interest since the complex structure is not available yet.

Previously, we identified a novel ubiquitin binding site on STAM1 VHS and suggested the binding mode of VHS-ubiquitin complex [14]. Also we reported the backbone resonance assignments for STAM1^{N191} which contains both the VHS domain and UIM, and showed that two ubiquitin binding domains are linked by very flexible extended loop regions [15]. Based on our previous studies, here we performed the NMR and ITC experiments to elucidate the simultaneous binding of VHS and UIM in STAM1 to ubiquitin.

The solution structure of STAM1 UIM was determined in aqueous solution in this work, suggesting the UIM is intrinsically α-helix in intact STAM1. The steady-state $^{1}H–^{15}N$ heteronuclear NOE experiment supported the presence of the structurally independent α-helix in UIM region of STAM1 [15]. The UIM structure of STAM1 resembled other UIM structure alone [22] or in ubiquitin complex [25]. NMR and ITC data showed that the binding interfaces are mainly the hydrophobic surfaces, Leu176, Ala179, and Ser183 from UIM and the hydrophobic surface centered at Ile44. Our result corresponds well with previous mutagenic studies of UIM on the effect of the hydrophobic residues in ubiquitin binding [26–29].

Although we were not able to measure the STAM1 UIM binding of ubiquitin in ITC experiments by using the synthetic peptide, the binding was obvious in NMR titration experiments. This is because the detectable time-scale in protein–protein interaction is very suitable for weak bindings in NMR spectroscopy.

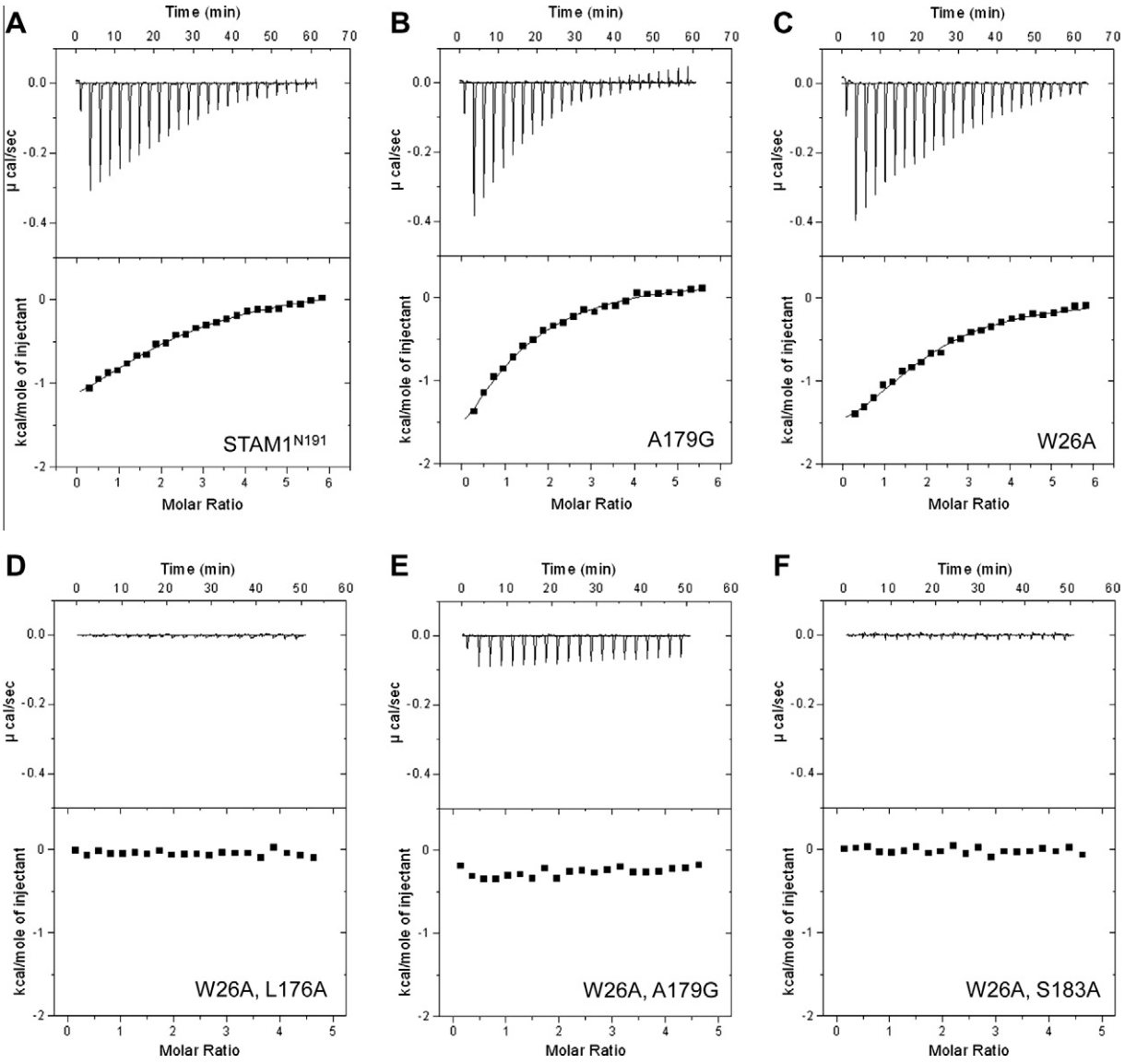

Fig. 4. Interaction between ubiquitin and the wild-type and mutant STAM1^{N191}. ITC data of STAM1^{N191} (A), STAM1^{N191}A179G (ubiquitin binding of VHS, B), and STAM1^{N191}W26A (ubiquitin binding of UIM, C) upon titration of ubiquitin. Ubiquitin binding affinities of double mutants, STAM1^{N191}W26AL176A (D), W26AA179G (E), and W26AS183A (E), were not measurable.

To measure exact ubiquitin binding affinity of UIM, we used the mutant STAM1 protein which lacks ubiquitin binding affinity of the VHS domain. The effect of UIM in STAM1 for ubiquitin binding was enhanced compared to that of UIM peptide (2.2 fold). The same tendency was also detected in the ubiquitin binding of the VHS domains. We suggest that the result in this work present more accurate binding aspect and physiological relevance in ubiquitin interaction.

Finally, the docking model of STAM1 UIM and ubiquitin complex was presented (see Supplementary data). The docking simulation was performed by using RosettaDock protocol. The complex structure of STAM1 UIM and ubiquitin (Supplementary Fig. S2C and D) showed the hydrophobic interaction provided by both central regions of UIM and ubiquitin as well as three putative hydrogen bond interactions. Even though the hydrophobic interaction plays crucial role in STAM1 UIM-ubiquitin binding, the electrostatic contribution is also significant (see Supplementary results).

In conclusion, we presented the first solution structure of STAM1 UIM and evaluated the individual ubiquitin binding affinity of the VHS domain and UIM motif in STAM1 with physiological relevance. This approach will be beneficial to understand the binding mode of ESCRT complex to polyubiquitin as well as the protein complex involved in multiple (or poly) ubiquitin binding domains.

Acknowledgments

This work was supported by a grant of the Korea Healthcare technology R&D Project, Ministry for Health & Welfare, Republic of Korea (A092006) to H-C. Ahn and partially supported by grants from the Functional Proteomics Center, th 21st Frontier Research & Development Program of the Korea Ministry of Science to E. E. KIM.

Appendix A. Supplementary data

Supplementary data associated with this article can be found, in the online version, at doi:10.1016/j.bbrc.2010.12.103.

References

[1] V. Kirkin, I. Dikic, Role of ubiquitin- and Ubl-binding proteins in cell signaling, Curr. Opin. Cell Biol. 19 (2007) 199–205.

[2] C.M. Pickart, D. Fushman, Polyubiquitin chains: polymeric protein signals, Curr. Opin. Chem. Biol. 8 (2004) 610–616.
[3] L. Hicke, R. Dunn, Regulation of membrane protein transport by ubiquitin and ubiquitin-binding proteins, Annu. Rev. Cell Dev. Biol. 19 (2003) 141–172.
[4] L. Hicke, Protein regulation by monoubiquitin, Nat. Rev. Mol. Cell Biol. 2 (2001) 195–201.
[5] Y. Mosesson, K. Shtiegman, M. Katz, Y. Zwang, G. Vereb, J. Szollosi, Y. Yarden, Endocytosis of receptor tyrosine kinases is driven by monoubiquitylation, not polyubiquitylation, J. Biol. Chem. 278 (2003) 21323–21326.
[6] A. Hershko, A. Ciechanover, The ubiquitin system, Annu. Rev. Biochem. 67 (1998) 425–479.
[7] F. Huang, D. Kirkpatrick, X. Jiang, S. Gygi, A. Sorkin, Differential regulation of EGF receptor internalization and degradation by multiubiquitination within the kinase domain, Mol. Cell 21 (2006) 737–748.
[8] L.M. Duncan, S. Piper, R.B. Dodd, M.K. Saville, C.M. Sanderson, J.P. Luzio, P.J. Lehner, Lysine-63-linked ubiquitination is required for endolysosomal degradation of class I molecules, EMBO J. 25 (2006) 1635–1645.
[9] C. Raiborg, H. Stenmark, The ESCRT machinery in endosomal sorting of ubiquitylated membrane proteins, Nature 458 (2009) 445–452.
[10] P.S. Bilodeau, S.C. Winistorfer, W.R. Kearney, A.D. Robertson, R.C. Piper, Vps27-Hse1 and ESCRT-I complexes cooperate to increase efficiency of sorting ubiquitinated proteins at the endosome, J. Cell Biol. 163 (2003) 237–243.
[11] D. Katzmann, C. Stefan, M. Babst, S. Emr, Vps27 recruits ESCRT machinery to endosomes during MVB sorting, J. Cell Biol. 162 (2003) 413–423.
[12] X. Ren, J.H. Hurley, VHS domains of ESCRT-0 cooperate in high-avidity binding to polyubiquitinated cargo, EMBO J. 29 (2010) 1045–1054.
[13] A. Lange, D. Hoeller, H. Wienk, O. Marcillat, J.M. Lancelin, O. Walker, NMR reveals a different mode of binding of the Stam2 VHS domain to ubiquitin and diubiquitin, Biochemistry (2010). Publication Date (Web): December 1, 2010, http://dx.doi.org/DOI:10.1021/bi101594a.
[14] Y.H. Hong, H.C. Ahn, J. Lim, H.M. Kim, H.Y. Ji, S. Lee, J.H. Kim, E.Y. Park, H.K. Song, B.J. Lee, Identification of a novel ubiquitin binding site of STAM1 VHS domain by NMR spectroscopy, FEBS Lett. 583 (2009) 287–292.
[15] J. Lim, Y.H. Hong, B.J. Lee, H.C. Ahn, Backbone ^{1}H, ^{13}C, and ^{15}N assignments for the tandem ubiquitin binding domains of signal transducing adapter molecule 1, Biomol. NMR Assign. (2010). Publication Date (Web): October 7, 2010, http://dx.doi.org/10.1007/s12104-010-9265-2.
[16] F. Delaglio, S. Grzesiek, G.W. Vuister, G. Zhu, J. Pfeifer, A. Bax, NMRPipe: a multidimensional spectral processing system based on UNIX pipes, J. Biomol. NMR 6 (1995) 277–293.
[17] B.A. Johnson, Using NMRView to visualize and analyze the NMR spectra of macromolecules, Methods Mol. Biol. 278 (2004) 313–352.
[18] K. Wüthrich, NMR of Protein and Nucleic Acids, Wiley, New York, 1986.
[19] J.P. Linge, S.I. O'Donoghue, M. Nilges, Automated assignment of ambiguous nuclear overhauser effects with ARIA, Methods Enzymol. 339 (2001) 71–90.
[20] A.T. Brunger, P.D. Adams, G.M. Clore, W.L. DeLano, P. Gros, R.W. Grosse-Kunstleve, J.S. Jiang, J. Kuszewski, M. Nilges, N.S. Pannu, R.J. Read, L.M. Rice, T. Simonson, G.L. Warren, Crystallography & NMR system: a new software suite for macromolecular structure determination, Acta Cryst. D 54 (1998) 905–921.
[21] R.A. Laskowski, J.A. Rullmannn, M.W. MacArthur, R. Kaptein, J.M. Thornton, AQUA and PROCHECK-NMR: programs for checking the quality of protein structures solved by NMR, J. Biomol. NMR 8 (1996) 477–486.
[22] R.D. Fisher, B. Wang, S.L. Alam, D.S. Higginson, H. Robinson, W.I. Sundquist, C.P. Hill, Structure and ubiquitin binding of the ubiquitin-interacting motif, J. Biol. Chem. 278 (2003) 28976–28984.
[23] K.E. Sloper-Mould, J.C. Jemc, C.M. Pickart, L. Hicke, Distinct functional surface regions on ubiquitin, J. Biol. Chem. 276 (2001) 30483–30489.
[24] B. Strack, A. Calistri, H.G. G?tlinger, Late assembly domain function can exhibit context dependence and involves ubiquitin residues implicated in endocytosis, J. Virol. 76 (2002) 5472–5479.
[25] K.A. Swanson, R.S. Kang, S.D. Stamenova, L. Hicke, I. Radhakrishnan, Solution structure of Vps27 UIM-ubiquitin complex important for endosomal sorting and receptor downregulation, EMBO J. 22 (2003) 4597–4606.
[26] E. Klapisz, I. Sorokina, S. Lemeer, M. Pijnenburg, A.J. Verkleij, P.M. van Bergen en Henegouwen, A ubiquitin-interacting motif (UIM) is essential for Eps15 and Eps15R ubiquitination, J. Biol. Chem. 277 (2002) 30746–30753.
[27] S. Polo, S. Sigismund, M. Faretta, M. Guidi, M.R. Capua, G. Bossi, H. Chen, P. De Camilli, P.P. Di Fiore, A single motif responsible for ubiquitin recognition and monoubiquitination in endocytic proteins, Nature 416 (2002) 451–455.
[28] S.C. Shih, D.J. Katzmann, J.D. Schnell, M. Sutanto, S.D. Emr, L. Hicke, Epsins and Vps27p/Hrs contain ubiquitin-binding domains that function in receptor endocytosis, Nat. Cell. Biol. 4 (2002) 389–393.
[29] T. Woelk, B. Oldrini, E. Maspero, S. Confalonieri, E. Cavallaro, P.P. Di Fiore, S. Polo, Molecular mechanisms of coupled monoubiquitination, Nat. Cell. Biol. 8 (2006) 1246–1254.
[30] R. Koradi, M. Billeter, K. Wüthrich, MOLMOL: a program for display and analysis of macromolecular structures, J. Mol. Graph 14 (1996) 51–55 (29–32).